

Insight into planktonic protistan and fungal communities across the nutrient-depleted environment of the South Pacific Subtropical Gyre

Katarina Kajan,^{1,2} Bernhard M. Fuchs,³ Sandi Orlic^{1,2}

AUTHOR AFFILIATIONS See affiliation list on p. 12.

ABSTRACT Ocean microorganisms constitute ~70% of the marine biomass, contribute to ~50% of the Earth's primary production, and play a vital role in global biogeochemical cycles. The marine heterotrophic and mixotrophic protistan and fungal communities have often been overlooked mainly due to limitations in morphological species identification. Despite the accumulation of studies on biogeographic patterns observed in microbial communities, our understanding of the abundance and distribution patterns within the microbial community of the largest subtropical gyre, the South Pacific Gyre (SPG), remains incomplete. Here, we investigated the diversity and vertical composition of protistan and fungal communities in the water column of the ultra-oligotrophic SPG. Our results showed apparent differences in protistan community diversity in the photic and aphotic regions. The entire protistan community diversity was significantly affected by temperature, salinity, oxygen, and nutrient concentrations, while the parasitic community diversity was also affected by chlorophyll *a* concentration. The parasitic protists were assigned to the class Syndiniales accounting for over 98% of the total parasitic protists, exhibiting higher relative sequence abundance along the water depth and displaying consistent patterns among different sampling stations. In contrast to the protistan community, the fungal community along the SPG primarily clustered based on the sampling station and pelagic zones. In particular, our study reveals a significant presence of parasitic protists and functionally diverse fungi in SPG and their potential impact on carbon cycling in the gyre.

IMPORTANCE Our findings carry important implications for understanding the distribution patterns of the previously unrecognized occurrence of parasitic protists and functionally diverse fungi in the nutrient-limited South Pacific Gyre. In particular, our study reveals a significant presence of parasitic Syndiniales, predominantly abundant in the upper 300 m of the aphotic zone in the gyre, and a distinct presence of fungal communities in the aphotic zone at the central part of the gyre. These findings strongly suggest that these communities play a substantial role in yet insufficiently described microbial food web. Moreover, our research enhances our understanding of their contribution to the dynamics of the food webs in oligotrophic gyres and is valuable for projecting the ecological consequences of future climate warming.

KEYWORDS South Pacific Subtropical Gyre, parasitic protists, fungi

In the marine environment, different microorganisms, including prokaryotes, protists, fungi, and viruses, have adapted to thrive in specific habitats, displaying a variety of forms, functions, and strategies (1, 2). These microorganisms constitute nearly 90% of the biomass and drive approximately 98% of primary production, playing a vital role in maintaining the structure and functioning of marine ecosystems (3–5). Studies have

Editor Jeffrey A. Gralnick, University of Minnesota
Twin Cities, St. Paul, Minnesota, USA

Address correspondence to Sandi Orlic, sorlic@irb.hr.

The authors declare no conflict of interest.

See the funding table on p. 12.

Received 4 August 2023

Accepted 18 January 2024

Published 9 February 2024

Copyright © 2024 Kajan et al. This is an open-access article distributed under the terms of the [Creative Commons Attribution 4.0 International license](https://creativecommons.org/licenses/by/4.0/).

indicated that marine protists contribute to around 50% of annual primary production, consuming nearly 66% of it and an additional 10% of bacterial primary production (2, 6). Marine protists form a diverse and heterogeneous community consisting of autotrophs (primary producers), heterotrophs (phagotrophs and parasites), and a wide range of lineages that exhibit different mixotrophic strategies (7, 8). These different functional groups occupy specific niches within the marine food web and play crucial roles in biogeochemical cycles encompassing the majority of eukaryotic diversity in the oceans (2, 9). In contrast, the significance of marine ecosystems as fungal habitats has often been neglected (10–12). Recent advancements in methodologies have shed light on the role of fungi in various aquatic systems, but a comprehensive conceptual framework is still lacking (13, 14). However, it has been proposed that fungi have the capacity to greatly influence the structure, stability, and functionality of marine food webs through symbiotic and parasitic interactions with other organisms and degradation of organic matter (15–17).

One significant feature of the marine ecosystem is the presence of subtropical gyres, which cover approximately 70% of the ocean surface (18). Although the primary production per unit of the surface within these gyres is relatively low (19–21), their extensive size contributes significantly to the overall ocean productivity and global biogeochemical cycles (22). The microbial community's activity, as revealed by both remote sensing and *in situ* measurements, plays a substantial role in shaping global biogeochemical cycles (23–26). Despite the numerous studies focusing on biogeographic patterns in marine ecosystems observed in microbial communities, our current understanding of the abundance and distribution patterns within the pelagic microbial community of the largest subtropical gyre, the South Pacific Gyre (SPG), remains limited. In contrast, numerous studies have been conducted in the water column of the open-ocean North Pacific Gyre, revealing the variety of microbial communities [i.e., references (27, 28)].

One of the sampling campaigns conducted in SPG was carried out at 15 stations along a transect from Antofagasta (Chile) to Wellington (New Zealand) during the R/V Sonne “UltraPac” cruise (SO245) in the Austral summer of 2015/2016 (Fig. 1). The most

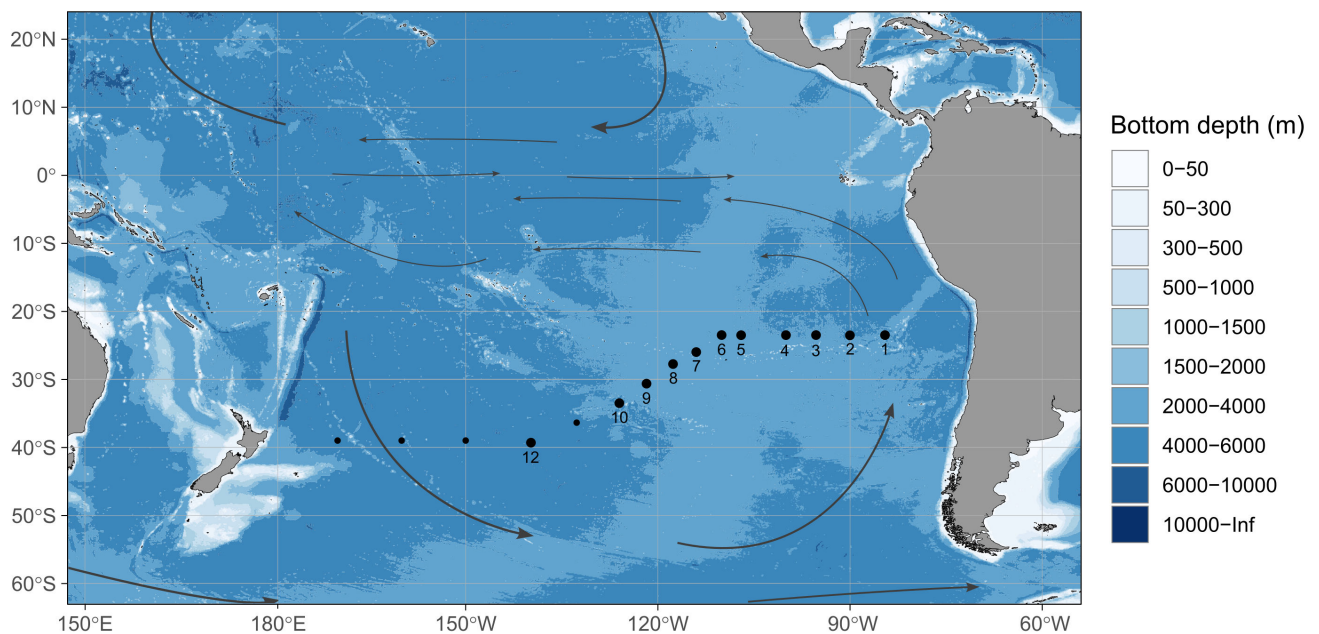


FIG 1 Map of sampling stations along the SO245 UltraPac transect. Black points denote sampling stations; samples used in the following study were collected at the enumerated dots. Gray arrows show the main ocean currents. The map was made in R and finished in Inkscape.

significant variations in physicochemical conditions were observed within the top 500 m of the SPG (Fig. S1) (29). In the central gyre region, surface water temperatures were consistently high, ranging between 20°C and 25°C (Fig. S1A). Chlorophyll fluorescence measurements indicated extremely low levels of primary productivity in the surface waters down to a depth of 70 m (Fig. S1B). The deep chlorophyll maximum (DCM) occurred between depths of 190 to 200 m, with a fluorescence reading of 0.5 $\mu\text{g L}^{-1}$. Previous studies conducted in the same sampling campaign have analyzed prokaryotic and phototrophic eukaryotic communities together with dissolved organic matter (29–32). We aimed to decipher the diversity and vertical distribution of protistan and fungal communities in the water column of the ultra-oligotrophic SPG across the longitudinal scale of 5,500 km. In the central gyre region, the additional water sampling was carried out within the vertical profile of 300 m over 24 hours to evaluate the variation in the day-night cycle (diel shifts) of the protistan and fungal communities. Using a DNA metabarcoding approach (18S rRNA gene and ITS2 region), our objectives were to (i) uncover the longitudinal- and depth-related distribution patterns of protistan and fungal community in the water column, (ii) detect which physicochemical parameters shape the protistan and fungal community composition, and (iii) evaluate the dynamic diel variations in community structure along the water column in the central gyre region.

RESULTS

Community composition, diversity, and assembly of protists along the SPG

Based on the 18S rRNA gene amplicon sequencing data analysis, the protists found at different depths and stations along the SPG were clustered into 1,288 amplicon sequence variants (ASVs). The final data set included samples above 300 m encompassing the epipelagic, DCM, and upper mesopelagic zone, along with samples collected during diel sampling at station 8 ($n = 84$). Remarkably, along the SPG, the relative sequence abundance of the protistan community at the supergroup level exhibited a striking similarity of community structure across longitudinal scales of 5,500 km (Fig. S2). The level of protistan diversity in the epipelagic zone was higher than below the DCM in terms of ASV richness and Shannon index, showing a negative correlation to water depth (Table S1; Fig. S3). The highest (367 ASVs) and lowest (109 ASVs) richness values occurred at station 5 at 50 m and station 7 at 300 m depth, respectively (Table S1). On the contrary, no significant difference was found in the protistan phylogenetic distance along the water depth (Fig. S3).

Alveolata dominated all analyzed samples, with an average relative sequence abundance of $\sim 92\% \pm 2\%$ within the protistan community per sampling station (Fig. S2). Other supergroups, such as Stramenopiles, did not exceed a relative sequence abundance of 18%. Within the Alveolata, the division Dinoflagellates contributed significantly to protistan community composition (Fig. S4), together with 83% of the total assigned ASVs demonstrating relatively high ASV richness (total ASV $n = 1,066$; Table S1). These prevalent ASVs were taxonomically affiliated at the class level as Dinophyceae and parasitic Syndiniales, comprising 40% (25%–61%) and 48% (25%–68%) of the total ASV number, respectively (Fig. 2; Table S1; Fig. S5). Dinophyceae reads were particularly abundant in the euphotic zone, exhibiting a negative correlation with depth (Fig. S5). In contrast, the relative sequence abundance of Syndiniales increased in the aphotic zone (Fig. S5). These depth-related patterns of the protistan community composition were further supported by clustering the relative sequence abundance of the protistan community at the order level based on the different irradiance zones [Fig. 2; permutational multivariate analysis of variance (PERMANOVA), $R^2 = 0.280$, $P = 0.001$].

On average, the protistan community accounted for 49% parasitic, 17% mixotrophic, 10% heterotrophic, and 5% photosynthetic protists in terms of functional groups (Fig. S6). Approximately, 18% of the community had unknown functions, primarily assigned only to the order level mainly to class Dinophyceae. Among the parasitic protists, 65% of the ASVs was found in both the euphotic and aphotic zones (Fig. 3A). However, a two-sample t -test revealed a significant difference in the relative sequence abundance of

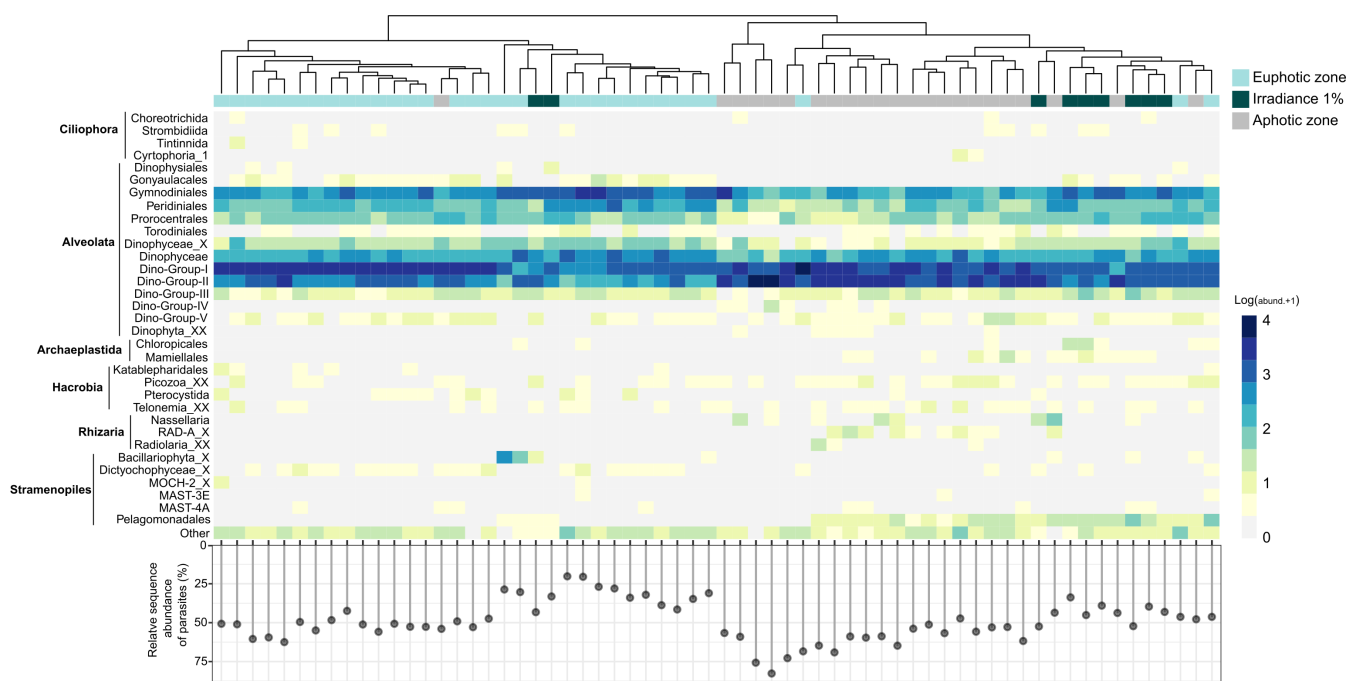


FIG 2 Partitioning of protistan major taxonomic groups by irradiance zone in South Pacific Gyre. Heatmap of relative sequence abundance of protistan community at the order level (orders with relative sequence abundance > 1%). Columns were clustered based on Bray-Curtis distance with the top row colored by irradiance zone. Abundances were log-transformed. Below the heatmap, the plot shows the relative sequence abundance of parasitic protists in clustered samples.

parasitic protists between the two zones with an average in the euphotic zone of 43.9% and in the aphotic zone of 58.5% (t -test, $df = 51.6$, $P < 0.001$; Table S1). The parasitic protists were represented by 667 ASVs assigned to the class Syndiniales, accounting for over 98% of the total parasitic protists. The remaining 2% of the ASVs was affiliated to parasitic protists Sagenista (*Labyrinthulomycetes*) and Ciliophora (*Oligohymenophorea*).

The parasitic Syndiniales encompassed five main groups at the order level: Dino-Groups I, II, III, IV, and V. The most abundant genera with high relative sequence abundance belonged to Dino-Groups I and II with 228 and 407 ASVs (Fig. 2; Table S1). Only the relative sequence abundance of Dino-Group II had a significant positive correlation with depth displaying consistent patterns among sampling stations (Fig. S7). In contrast, Dinophyceae had twofold less ASVs and a lower contribution of highly dominant genera to the overall protistan community (Table S1). At the order level, the most abundant with the highest relative sequence abundance were Gymnodiniales (15%), Peridinales (7%), and Procentrales (5%) (Fig. 2).

The PCoA conducted at the ASV level demonstrated that the entire protistan community inhabiting the SPG primarily clustered based on sampling depth, exhibiting a distinct separation between the euphotic and aphotic zones (Fig. 3B). This result was further supported by PERMANOVA analysis, where sampling depth accounted for 42% of the variation of ASV composition, while the irradiance zone and sampling station contributed 19% each (Table S2). Notably, similar to the overall protistan community, the differences in sampling depth had a more pronounced impact on the structure of parasitic protists compared with zonal differences, confirming the significant influence of vertical physicochemical gradients on the overall composition of the protistan community.

The distance decay model was applied to identify the factors influencing the protistan diversity. The analysis revealed a significant similarity decline within the entire protistan and parasitic community as geographic distance increased ($R^2 = 0.019$, $P < 0.001$; Fig. S8A; $R^2 = 0.036$, $P < 0.001$; Table S3). Furthermore, linear regression models demonstrated

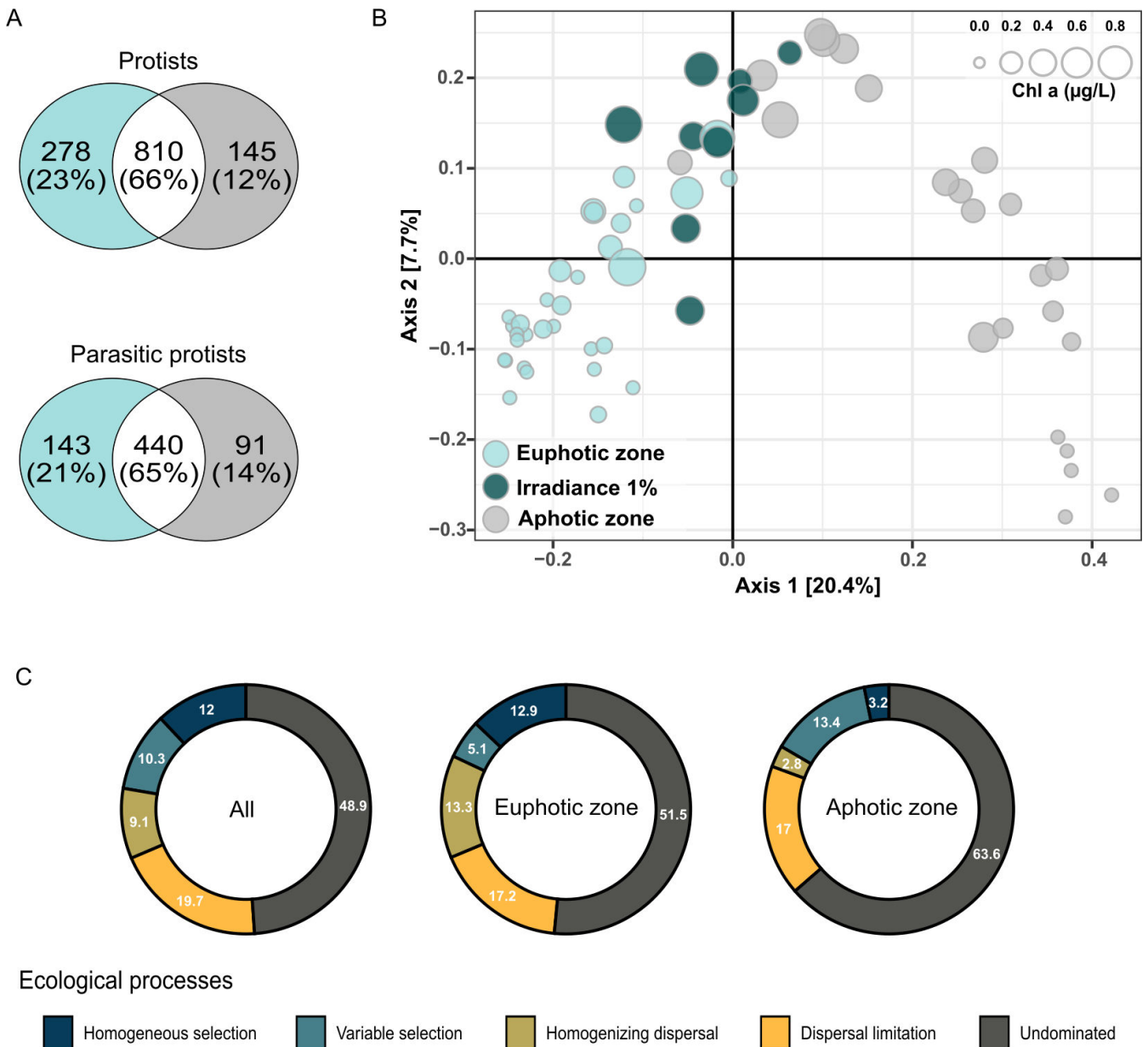


FIG 3 Vertical differences in the protistan community in South Pacific Gyre. (A) Number of unique, shared, and ubiquitous ASVs of all protists and parasitic protists across the photic and aphotic zones. Color-coded categories by irradiance zone (photic and aphotic zone). (B) Principal coordinate analysis (PCoA) of protistan community diversity color coded by irradiance zones, including irradiance zone of 1%. Each point represents an individual sample, and the circle size indicates the chlorophyll *a* concentration. (C) Relative importance of ecological processes driving the protistan assembly in SPG across the entire, euphotic, and aphotic zones.

that environmental differences had a stronger impact on the community structure diversity of the entire and parasitic protistan community compared with geographical distance ($R^2 = 0.313, P < 0.001; R^2 = 0.194, P < 0.001$; Table S3). The Mantel analysis was performed with various environmental factors to elucidate further the environmental drivers of protistan variation (Fig. S8B; Table S4). Results showed that the entire protistan community composition was significantly affected by temperature, salinity, oxygen, and nutrient concentrations, while the parasitic community additionally changed with chlorophyll *a* concentration (Table S4).

Whether the interplay of assembly processes governing the protistan community turnover varies in the euphotic and aphotic zone, the null model was applied (Fig. S9).

The ecological processes across both zones of the SPG were dominated by dispersal limitation together with a higher influence of homogenizing dispersal and homogeneous selection in the euphotic zone (Fig. 3C). A great proportion of the processes was undominated (51%–63%).

Diel variation of the protistan community composition

Evaluating the diel variation of the protistan community composition within the vertical profile of 300 m at the oligotrophic station in the central area of SPG (station 8), our results have shown that samples collected at the same depth at different time points have similar community structure while also showing the difference in irradiance zones (PERMANOVA; Fig. S10; Table S5). The significant inter-depth differences in protistan community structure were observed among communities at 50 m and 200 m and 100 m and 200 m, respectively [analysis of variance (ANOVA), $P < 0.05$; Fig. S11].

The overall protistan community was predominantly composed of Alveolata (Dinoflagellata) across all samples (Fig. S11). A high negative correlation was shown between the relative sequence abundance of Syndiniales and Dinophyceae (Pearson's correlation $R = -0.97$, $P < 0.001$). At station 8, Syndiniales were highly represented by Dino-Group I and Dino-Group II (Fig. S13). Within Dino-group I, clades 1 and 5 accounted for higher proportions than others, while clades 10 and 11 and 22 were the predominant clades in Dino-Group II. The relative sequence abundance of Dino-Group II exhibited a sharp increase in depth (Pearson's correlation $R = 0.88$, $P < 0.001$). Dinophyceae were highly represented with Gymnodiniales and Peridiniales with the highest abundance at the surface (20 m; Fig. S13). The trophic functional groups exhibited contrasting distribution in diel depth variation (Fig. 4). The abundance of heterotrophic, mixotrophic, and photosynthetic protists reached the maximal relative sequence abundance in the euphotic zone, while parasitic communities in the aphotic zone (Fig. 4).



FIG 4 Diel variability in relative sequence abundance of protistan trophic functional groups at order level based on 18S rRNA gene amplicon sequencing data in the central gyre region at station 8 in the vertical profile of 300 m over 24 hours at four time points: 2 a.m., 8 a.m., 2 p.m., and 9 p.m.

To distinguish diel patterns within the protistan community, the dynamic variations in protistan community structure in each sampled depth were evaluated based on the coefficient of variation (CV) within alpha diversity and relative sequence abundance at order and functional group levels (Fig. S14 to S16).

Community composition and diversity of fungi along the SPG

Based on the ITS2 region, the relative sequence abundance of fungi was comparatively low to those of unidentified and unclassified, except for station 6 (Fig. S16). At station 6, the relative sequence abundance of fungi exceeded over 75% with vertical distribution across the mesopelagic and bathypelagic zones. For further analyses of the fungal community, a data set comprising 51 samples and 69 ASVs was used (constitutes 62% of the total ASVs assigned to fungi).

The main phyla contributing to the fungal diversity of the SPG were Ascomycota, Basidiomycota, and Mortierellomycota, with 20, 47, and 2 ASVs, respectively (Fig. 5A). ASVs assigned to Basidiomycota exhibited high relative sequence abundances in most samples, while Ascomycota had higher relative sequence abundance at sampling stations 7, 8, 10 and 12. In contrast to the majority of samples, the fungal community in the central part of SPG (station 6) was present in all depths dominated by the genus *Rhodotorula* (Microbotryomycetes). A considerable fraction of the phylotypes assigned using FUNGuild were classified as phototrophs, while 37% of ASVs represented saprotrophs and symbiotrophs (Fig. S17).

In contrast to the protistan community, the PCoA analysis showed that the fungal community along the SPG primarily clustered based on the sampling station and pelagic zones (Fig. 5B; Table S6). The site-specific diversity was confirmed with a higher distance decay relationship of fungal diversity and geographical distance in comparison to the protistan community ($R^2 = 0.166$, $P < 0.001$; Fig. 5C; Table S7). Conversely, the linear regression model demonstrated low environmental differences contributing to fungal diversity ($R^2 = 0.018$, $P < 0.001$; Table S7). Nevertheless, parameters such as oxygen, nitrates, phosphates, and temperature, unlike salinity and chlorophyll *a*, strongly affected the fungal diversity (Fig. 5D; Table S8).

Further analysis of fungal diversity and environmental parameters at station 6 revealed no significant correlations. Due to the relatively low relative sequence abundance of fungal ASVs, the diel variation of the community based on the ITS2 region was not further analyzed.

DISCUSSION

This study provides new insights into the vertical and longitudinal distribution of taxonomic and functional composition of protists and fungi along the subtropical South Pacific Gyre.

Taking place during the Australian summer, the research cruise covered a vast geographical area of 7,000 km along the SPG, conducting sampling that spanned the entire vertical profile from the surface to the depths of the bathypelagic waters. Our study comprised samples within the longitudinal scale of 5,500 km in which we analyzed the diversity and composition of the protistan and fungal community using 18S and ITS regions, respectively.

The similarity analysis revealed significant differences in the oceanic protist community regarding water depth. Depth was identified as a major driver of protist community composition, which aligns with previous studies (28, 33–36). The distribution pattern of protists closely resembled that of the bacterial community diversity studied in the same period within the SPG (29). Notably, the composition of the bacterial community exhibited substantial changes with increasing depth, primarily driven by variation in light variability (29). The most pronounced shifts in bacterial composition occurred in the 1% irradiance zone, characterized by a decline in the abundance of mesopelagic clades (29). A prior study on photosynthetic microbial communities found that the photosynthetic

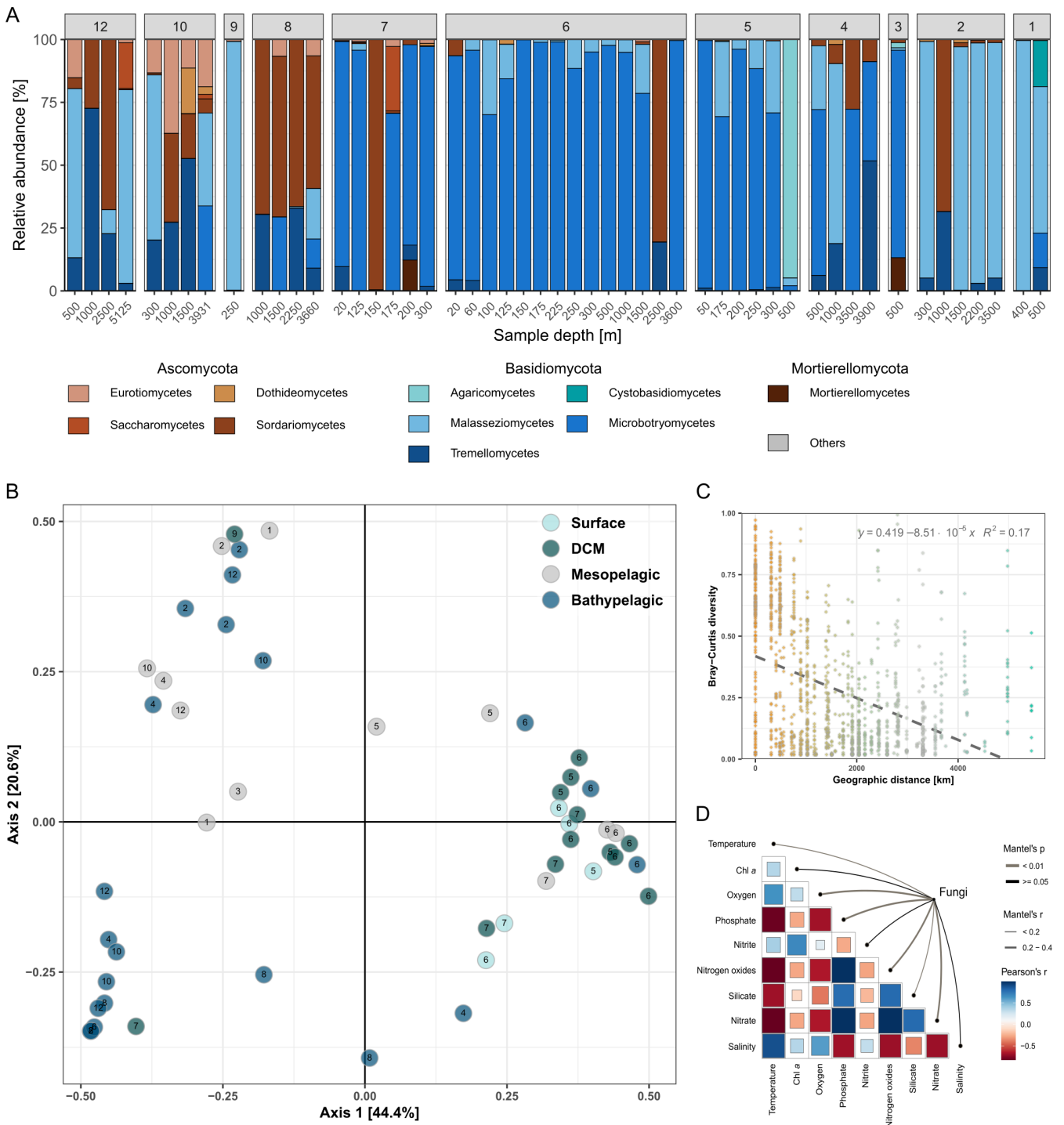


FIG 5 Partitioning of fungal major taxonomic groups and driving factors in South Pacific Gyre. (A) Relative sequence abundance of fungal classes per depth and sampling station. Classes with relative sequence abundance < 1% were aggregated into the group reported as “Others.” (B) PCoA of fungal community diversity color coded by pelagic zones and number coded by the station. Pelagic zones: epipelagic (surface: 20–80 m, DCM: 100–250 m); mesopelagic: 300–500 m; and bathypelagic: 1,000–5,125 m. (C) Distance-decay relationship of Bray-Curtis and geographical distance (km) between sampling stations of fungal community at the ASV level ($P < 0.001$). The line represents a linear regression. (D) Mantel test correlation plot of fungi with environmental variables based on the Bray-Curtis distance.

community primarily comprised *Prochlorococcus*, aerobic anoxygenic phototrophs, and a diverse community of small photosynthetic eukaryotes. Surprisingly, photosynthetic activity spanned the euphotic zone rather than concentrated solely at the DCM, with

68%–79% of primary productivity occurring above DCM (32) aligning with our observation.

In this study, we found significant correlations between environmental variables and protistan diversity, highlighting the impact of abiotic factors on community dynamics within the upper 300 m of the water column. Our results indicate that protistan diversity is primarily influenced by temperature and nitrogen availability rather than other environmental factors or geography. These results are consistent with the vertical stratification of microbial communities, which respond to changes in physicochemical parameters, such as light, temperature, and nutrient availability (37). Notably, the extremely low concentrations of inorganic nitrogen throughout the euphotic zone indicate the importance of nutrient recycling for primary production in the SPG. This emphasizes the crucial role of heterotrophic activities responsible for the breakdown and recycling of organic matter (32).

Dinoflagellates exhibit diverse metabolic capabilities, including photosynthetic, mixotrophic, and heterotrophic (parasitic). This versatility allows dinoflagellates to contribute to the export of organic matter through their photosynthetic activities in the euphotic zone and the remineralization processes within the mesopelagic zone within the same regional environment (38).

The aphotic zone of the SPG exhibited a greater prevalence of parasitic communities, indicating their heightened contribution to the overall ecosystem. However, despite the differences in relative sequence abundances, there was also a notable similarity between the communities. This similarity suggests that ecologically and morphologically similar species have likely partitioned their ecological niches, allowing for their coexistence in the region. A high prevalence of parasitic protists was also recorded in our diel sampling, with the highest contribution of Syndiniales. Their wide distribution and genetic diversity due to their ability to colonize a wide range of ecological niches, which was also represented in our results (39–43). Parasitism is an important source of mortality within marine protist communities, though it is seldom accounted for in ecosystem and biogeochemical models (44).

Additionally, previous research has shown that the mesopelagic zone exhibits high metabolic activity among protists and approximately 90% of carbon is respired in this particular layer. Syndiniales, highly abundant in our samples, appear to have a significant role as parasites in SPG food webs, although this interaction has been overlooked. This suggests a potential feedback mechanism between parasitic infections, the release of organic matter, and prokaryotic assimilative activity. The capacity of these parasitoids to control their hosts depends on their parasitic fitness and mechanisms that determine parasitic specificity (45, 46). Host density is thought to be the main determinant of parasite abundance and infection rates, with increased host encounters and infections occurring under conditions of a plankton bloom. Other factors may influence Syndiniales population dynamics, such as temperature, nutrients, water column depth, and degree of physical mixing, although these factors have not been studied extensively. In addition, zoosporic parasites likely play a significant role in maintaining genetic polymorphism and biodiversity in host populations and regulating phytoplankton succession. They can infect several types of plankton including protozoan, such as dinoflagellates or ciliates, and metazoans, such as crustaceans and copepods as endoparasites (47). Because of their short generation times and abundant progeny, zoosporic parasitoids exert important top-down control that significantly influences the entire aquatic food webs, especially phytoplankton population dynamics. Our limited diel resolution makes it difficult to identify reliable factors influencing Syndiniales populations under different ecological and biological conditions (48).

The global planktonic marine fungal community has been found to cluster by the ocean, suggesting that fungal dispersal occurs in oceans (49, 50). Fewer studies have focused on planktonic fungi in the open ocean compared with coastal regions, and even fewer have targeted the mesopelagic zone and below. Our results have shown the clustering of fungal communities among the sites and confirmed that site-to-site

variation was a stronger factor in explaining fungal community structure, suggesting that local environmental filtering may play a critical role in assembling the fungal community in SPG (50). The homogeneous fungal community patterns observed in ultra-oligotrophic sampling station 6, the “oligotrophic eye,” reflect surprisingly stable community composition across the vertical depth profile from 20 to 3,600 m. The typically oligotrophic conditions would suggest low abundance of pelagic fungi, which may increase under eutrophication or dissolved organic carbon enrichment, as observed for copiotrophic bacteria. Although few studies have tried to quantify the actual biomass of fungi, it seems it could exceed that of bacteria, particularly in habitats rich in organic carbon (51–53). Additionally, the fungal community in the SPG inhabiting the aphotic realm was found to be closely related to especially oxygen and nitrate concentrations. The prevalent genus *Rhodotorula* detected in the SPG is the predominant basidiomycetes usually found in the marine environments such as seawater, sediment, and hydrothermal vent, and also as symbionts of marine invertebrates and seaweeds (51, 54, 55). New studies of deep-sea sediment fungi isolates in SPG have shown their metabolic capability of degradation of aromatic compounds, lignin, lignocellulose, carbonate, and carboxylic acids (56).

Conclusions

Our study provides evidence of the previously unrecognized occurrence of parasitic protists and functionally diverse fungi in the nutrient-limited South Pacific Gyre. In this work, we have analyzed the protistan community focusing on the significant presence of parasitic Syndiniales, which were found to be particularly abundant in the upper 300 m of the aphotic zone in the SPG. Additionally, our analysis of fungal communities revealed their distinct presence in the aphotic zone at the central part of the SPG, suggesting their substantial contribution to the yet insufficiently described microbial food web. To draw broader conclusions, additional samplings are required to ensure significant reliability and enhance the applicability of our findings. Exploring the diversity of fungi and their interactions with protistan and prokaryotic communities will enable us to understand open ocean ecosystems comprehensively.

MATERIALS AND METHODS

Field sampling

A transect along the South Pacific Ocean covered a length of 7,000 km and a depth of up to 5,000 m. Sampling was carried out at 15 stations along a transect from Antofagasta (Chile) to Wellington (New Zealand) during the R/V Sonne “UltraPac” cruise (SO245) in the Austral summer from 17 December 2015 to 28 January 2016 (Fig. 1). The detailed sampling strategy, physicochemical measurements, and nucleic acid extraction methods are described by Reintjes et al. (29). Physical oceanography, oxygen, and nutrient data are available via the Pangea database (57, 58). The samples used in this study are listed and described in Table S9. Briefly, a total of 152 seawater samples were collected from multiple depths at 11 stations, including five intermediate stations: 1, 3, 5, 7, and 9, and six main stations: 2, 4, 6, 8, 10, and 12. Six sampling stations covered the central gyre region (stations 4–9; SPG), three sampling stations on the northern east side of the gyre (Southeast Pacific), and two stations in the Southwest Pacific. In total, 8 samples were collected throughout the water column on the intermediate stations in the range of 20 to 500 m, while 12 to 15 samples were collected on the main stations with a maximum depth of 50 to 100 m above the seafloor. Water sampling encompassed epipelagic (surface: 20–80 m, DCM: 100–250 m), mesopelagic (300–500 m), and bathypelagic zones (1,000–5,125 m). The depth of the irradiance zones (photic, irradiance of 1%, and aphotic zone) varied between the sampling stations. The depth of the zone with irradiance of 1% varied between 162 m in the SPG (stations 4 to 9), 110 m in station 1, and 94 m in station 12.

In the central gyre region at station 8, the additional water sampling was carried out within the vertical profile of 300 m over 24 hours to evaluate the variation in the day-night cycle (diel shifts) of the protistan and fungal communities. Water samples at nine depths were collected at four time points: 2 a.m., 8 a.m., 2 p.m., and 9 p.m.

Amplicon sequencing and analysis

The V4 region of the 18S rRNA gene was amplified with primers TAREuk454FWD1 and TAREukREV3 (59) and the ITS2 region of the fungal rRNA gene with primer pair ITS3-Mix1-Mix2 (TCCTCCGCTTAyTgATAtGc), a modified ITS3 Mix2 forward primer ITS3-mkmix2 (CAWCGATGAAGAACGCAG) (60), and a reverse primer ITS4 [equimolar mix of cwmix1 (TCCTCCGCTTAyTgATAtGc) and cwmix2 (TCCTCCGCTTAtTrATAtGc)] (61), using a unique dual-barcoding two-step PCR approach (UDB-H12) as described by Pjevac et al. (62). Amplicons were sequenced in a paired-end mode (2 × 300 bp) on a MiSeq platform (Illumina, San Diego, CA, USA) at the Joint Microbiome Facility of the Medical University of Vienna and the University of Vienna. Details on sequence trimming and settings for quality filtering are described by Pjevac et al. (62). Sequence data were processed in R (63) using DADA2 following the workflow by Callahan et al. (64) in a pooled mode using all amplicon libraries per sequencing run. Taxonomic assignment was done by mapping 18S V4 ASV sequences against the PR2 reference database (v.4.12.0) (65) and ITS2 ASV sequences against the UNITE reference database (v. 04.02.2020) (66). The ASVs assigned to the protistan taxon at the taxonomic level “Division” were extracted from the 18S V4 data set, and the fungal taxon at the taxonomic level “Kingdom” extracted from the ITS2 data set was kept for further statistical analysis and data visualization. The functional groups were assigned based on the taxonomical classification of protistan ASVs into autotrophs, mixotrophs, parasites, osmotrophs, and phagotrophs. The functional assignment was determined according to Adl et al. (67) and the literature review (68, 69). The identified fungal taxa were assigned to functional groups with the FUNGuild tool (70) into pathotrophs, saprotrophs, symbiotrophs, etc. ASVs that did not match any taxa in the database were categorized as “Unknown.”

Statistical analysis and data visualization

All analyses and visualizations were performed with R v 4.2.2 (63) in R studio using packages phyloseq (71), tidyverse (72), vegan (73), ggplot2 (74), pheatmap (75), ggVennDiagram (76), picante (77), linkET (78), enmSdm (79), and geosphere (80). Prior to analyses, the standardization method of the ASV tables was applied according to Gutiérrez-Rodríguez et al. (81). Samples collected during diel sampling at station 8 with four time points (2 a.m., 8 a.m., 2 p.m., and 9 p.m.) were analyzed separately. Specifically, only samples obtained at 2 p.m. at station 8 were included for comparison with those from other stations.

The alpha diversity was estimated as the richness, Shannon-Wiener index, and Faith's phylogenetic distance computed using packages vegan and picante (73, 77). The phylogenetic tree of the protistan community was generated using Clustal Omega (82) for alignment and FastTree (83) to estimate phylogeny. Pearson's correlation was used to measure the strength of the linear relationship between relative sequence abundance and each predictor variable. PCoA was performed on the Bray-Curtis distance matrix at the level of protistan and fungal ASV. Prior to beta diversity analysis, Hellinger transformation was applied to the community composition data sets. To test for the compositional differences of protistan and fungal communities between the sampling station, depth, and irradiance zone among the samples, a PERMANOVA was run with 999 permutations using the function *adonis2* in package vegan (73). Using linear regression, the distance-decay relationship was evaluated by comparing the Bray-Curtis community distance matrix of protistan and fungal communities with geographic (km) and environmental distance. The geographic distance matrix was measured between the geographical location of sampling stations [package enmSdm (79) and geosphere (80)]. The Mantel test was used to determine the driving environmental factors (Euclidean

distance) on protistan and fungal community diversity based on the Bray-Curtis community distance matrix [linkET package (78)].

To evaluate the dynamic variation in community composition in each depth in the central gyre region at station 8, the CV was calculated. The average diel beta diversity based on the Bray-Curtis distance of community composition was calculated to obtain information on the inter- and intra-depth variabilities at four time points. The depth differences were tested by one-way ANOVA, followed by Tukey's multiple comparison tests.

Quantifying influences of ecological processes

The biodiversity ecological null model was used to evaluate processes driving protistan assembly (84, 85). Based on the standardized abundance ASV table and amplicon phylogenetic tree, the β -nearest taxon index (β NTI) of the protistan community was calculated. In order to test if there was a significant difference between molecular and phylogenetic turnover between the observed protistan assemblages, the β -mean nearest taxon index (β MNTD) was calculated. Further, the β NTI was calculated as the difference between the observed β MNTD and the null distribution. Deterministic processes (variable or homogeneous selection) are dominated when β NTI is greater than 2 or less than -2 . Values within the $2 > \text{NTI} > -2$ range indicate the dominance of stochastic processes (homogenizing dispersal or dispersal limitation) or random drift. Based on the sequence abundance of the protistan community, the Raup-Crick (RC) beta diversity was calculated to distinguish stochastic processes. Assemblages were structured by dispersal limitation if $\text{RC} > +0.95$, homogenizing dispersal if $\text{RC} < -0.95$, or random processes acting alone to undominated if RC falls between -0.95 and $+0.95$.

ACKNOWLEDGMENTS

We gratefully acknowledge Captain Mallon and the crew of the RV Sonne for their support and commitment throughout the expedition.

The UltraPac Expedition (SO245) was funded by the Federal Ministry of Education and Research of Germany (grant 03G0245A). This research was partially supported under the project STIM-REI, Contract Number: KK.01.1.1.01.0003, a project funded by the European Union through the European Regional Development Fund—the Operational Programme Competitiveness and Cohesion 2014–2020 (KK.01.1.1.01).

AUTHOR AFFILIATIONS

¹Division of Materials Chemistry, Ruđer Bošković Institute, Zagreb, Croatia

²Center of Excellence for Science and Technology-Integration of Mediterranean Region (STIM), Zagreb, Croatia

³Department of Molecular Ecology, Max Planck Institute for Marine Microbiology, Bremen, Germany

AUTHOR ORCIDs

Katarina Kajan  <http://orcid.org/0000-0002-9266-7245>

Bernhard M. Fuchs  <http://orcid.org/0000-0001-9828-1290>

Sandi Orlić  <http://orcid.org/0000-0002-6339-4145>

FUNDING

Funder	Grant(s)	Author(s)
EC European Regional Development Fund (ERDF)	KK.01.1.1.01.0003	Katarina Kajan Sandi Orlić

AUTHOR CONTRIBUTIONS

Katarina Kajan, Data curation, Formal analysis, Visualization, Writing – original draft | Bernhard M. Fuchs, Funding acquisition, Project administration, Writing – review and editing | Sandi Orlić, Conceptualization, Funding acquisition, Investigation, Project administration, Supervision, Writing – review and editing

DATA AVAILABILITY

The raw reads of the 18S rRNA gene and ITS2 region amplicon sequencing were deposited to the NCBI Sequence Read Archive (SRA) database under the BioProject accession number [PRJNA1051843](https://www.ncbi.nlm.nih.gov/bioproject/PRJNA1051843).

ADDITIONAL FILES

The following material is available [online](#).

Supplemental Material

Supplemental figures (Spectrum03016-23-s0001.docx). Figures S1 to S18.

Supplemental tables (Spectrum03016-23-s0002.xlsx). Tables S1 to S9.

REFERENCES

1. Stocker R. 2012. Marine microbes see a sea of gradients. *Science* 338:628–633. <https://doi.org/10.1126/science.1208929>
2. Worden AZ, Follows MJ, Giovannoni SJ, Wilken S, Zimmerman AE, Keeling PJ. 2015. Rethinking the marine carbon cycle: factoring in the multifarious lifestyles of microbes. *Science* 347:1257594. <https://doi.org/10.1126/science.1257594>
3. Caron DA. 2005. Marine microbial ecology in a molecular world: what does the future hold? *Sci Mar* 69:97–110. <https://doi.org/10.3989/scimar.2005.69s197>
4. Sogin ML, Morrison HG, Huber JA, Welch DM, Huse SM, Neal PR, Arrieta JM, Herndl GJ. 2006. Microbial diversity in the deep sea and the underexplored “rare biosphere.” *Proc Natl Acad Sci USA* 103:12115–12120. <https://doi.org/10.1073/pnas.0605127103>
5. Polimene L, Sailley S, Clark D, Mitra A, Allen JI. 2017. Biological or microbial carbon pump? The role of phytoplankton stoichiometry in ocean carbon sequestration. *J Plankton Res* 39:180–186. <https://doi.org/10.1093/plankt/fbw091>
6. Calbet A, Landry MR. 2004. Phytoplankton growth, microzooplankton grazing, and carbon cycling in marine systems. *Limn & Ocean* 49:51–57. <https://doi.org/10.4319/lo.2004.49.1.0051>
7. Caron David A., Alexander H, Allen AE, Archibald JM, Armbrust EV, Bachy C, Bell CJ, Bharti A, Dyrman ST, Guida SM, Heidelberg KB, Kaye JZ, Metzner J, Smith SR, Worden AZ. 2017. Probing the evolution, ecology and physiology of marine protists using transcriptomics. *Nat Rev Microbiol* 15:6–20. <https://doi.org/10.1038/nrmicro.2016.160>
8. Mitra A, Flynn KJ, Tillmann U, Raven JA, Caron D, Stoecker DK, Not F, Hansen PJ, Hallegraeff G, Sanders R, Wilken S, McManus G, Johnson M, Pitta P, Våge S, Berge T, Calbet A, Thingstad F, Jeong HJ, Burkholder JA, Glibert PM, Granéli E, Lundgren V. 2016. Defining planktonic protist functional groups on mechanisms for energy and nutrient acquisition: incorporation of diverse mixotrophic strategies. *Protist* 167:106–120. <https://doi.org/10.1016/j.protis.2016.01.003>
9. Caron DA, Countway PD, Jones AC, Kim DY, Schnetzer A. 2012. Marine protistan diversity. *Ann Rev Mar Sci* 4:467–493. <https://doi.org/10.1146/annurev-marine-120709-142802>
10. Amend A, Burgaud G, Cunliffe M, Edgcomb VP, Ettinger CL, Gutiérrez MH, Heitman J, Hom EFY, Ianiri G, Jones AC, Kagami M, Picard KT, Quandt CA, Raghukumar S, Riquelme M, Stajich J, Vargas-Muñiz J, Walker AK, Yarden O, Gladfelter AS. 2019. Fungi in the marine environment: open questions and unsolved problems. *mBio* 10:e01189-18. <https://doi.org/10.1128/mBio.01189-18>
11. Sen K, Sen B, Wang G. 2022. Diversity, abundance, and ecological roles of planktonic fungi in marine environments. *J Fungi (Basel)* 8:491. <https://doi.org/10.3390/jof8050491>
12. Breyer E, Baltar F. 2023. The largely neglected ecological role of oceanic pelagic fungi. *Trends Ecol Evol* 38:870–888. <https://doi.org/10.1016/j.tree.2023.05.002>
13. Grossart H-P, Van den Wyngaert S, Kagami M, Wurzbacher C, Cunliffe M, Rojas-Jimenez K. 2019. Fungi in aquatic ecosystems. *Nat Rev Microbiol* 17:339–354. <https://doi.org/10.1038/s41579-019-0175-8>
14. Cunliffe M. 2023. Who are the marine fungi?. *Environ Microbiol* 25:131–134. <https://doi.org/10.1111/1462-2920.16240>
15. Morales SE, Biswas A, Herndl GJ, Baltar F. 2019. Global structuring of phylogenetic and functional diversity of pelagic fungi by depth and temperature. *Front Mar Sci* 6:1–12. <https://doi.org/10.3389/fmars.2019.00131>
16. Gladfelter AS, James TY, Amend AS. 2019. Marine fungi. *Curr Biol* 29:R191–R195. <https://doi.org/10.1016/j.cub.2019.02.009>
17. Heitger M, Baltar F. 2023. Respiration, production, and growth efficiency of marine pelagic fungal isolates. *J Fungi (Basel)* 9:417. <https://doi.org/10.3390/jof9040417>
18. Roshan S, DeVries T. 2017. Efficient dissolved organic carbon production and export in the oligotrophic ocean. *Nat Commun* 8:2036. <https://doi.org/10.1038/s41467-017-02227-3>
19. Signorini SR, Franz BA, McClain CR. 2015. Chlorophyll variability in the oligotrophic gyres: mechanisms, seasonality and trends. *Front Mar Sci* 2. <https://doi.org/10.3389/fmars.2015.00001>
20. Sharma P, Marinov I, Cabre A, Kostadinov T, Singh A. 2019. Increasing biomass in the warm oceans: unexpected new insights from SeaWIFS. *Geophys Res Lett* 46:3900–3910. <https://doi.org/10.1029/2018GL079684>
21. Morel A, Gentili B, Claustre H, Babin M, Bricaud A, Ras J, Tièche F. 2007. “Optical properties of the “clearest” natural waters”. *Limn & Ocean* 52:217–229. <https://doi.org/10.4319/lo.2007.52.1.0217>
22. Claustre H, Huot Y, Obernosterer I, Gentili B, Tailliez D, Lewis M. 2008. Gross community production and metabolic balance in the South Pacific gyre, using a non intrusive bio-optical method. *Biogeosciences* 5:463–474. <https://doi.org/10.5194/bg-5-463-2008>
23. Carr M-E, Friedrichs MAM, Schmeltz M, Noguchi Aita M, Antoine D, Arrigo KR, Asanuma I, Aumont O, Barber R, Behrenfeld M, et al. 2006. A comparison of global estimates of marine primary production from ocean color. *Deep Sea Res Part II: Top Studies Ocean* 53:741–770. <https://doi.org/10.1016/j.dsr2.2006.01.028>

24. Longhurst A, Sathyendranath S, Platt T, Caverhill C. 1995. An estimate of global primary production in the ocean from satellite radiometer data. *J Plankton Res* 17:1245–1271. <https://doi.org/10.1093/plankt/17.6.1245>
25. Guidi L, Chaffron S, Bittner L, Eveillard D, Larhlimi A, Roux S, Darzi Y, Audic S, Berline L, Brum JR, et al. 2016. Plankton networks driving carbon export in the oligotrophic ocean. *Nature* 532:465–470. <https://doi.org/10.1038/nature16942>
26. McClain CR, Signorini SR, Christian JR. 2004. Subtropical gyre variability observed by ocean-color satellites. *Deep Sea Res Part II: Topical Stud Ocean* 51:281–301. <https://doi.org/10.1016/j.dsr2.2003.08.002>
27. Wu PF, Li DX, Kong LF, Li YY, Zhang H, Xie ZX, Lin L, Wang DZ. 2020. The diversity and biogeography of microeukaryotes in the euphotic zone of the northwestern Pacific ocean. *Sci Total Environ* 698:134289. <https://doi.org/10.1016/j.scitotenv.2019.134289>
28. Ollison GA, Hu SK, Mesrop LY, DeLong EF, Caron DA. 2021. Come rain or shine: depth not season shapes the active protistan community at station ALOHA in the North Pacific subtropical gyre. *Deep Sea Research Part I: Ocean Res Papers* 170:103494. <https://doi.org/10.1016/j.dsr.2021.103494>
29. Reintjes G, Tegetmeyer HE, Bürgisser M, Orlić S, Tews I, Zubkov M, Voß D, Zielinski O, Quast C, Glöckner FO, Amann R, Ferdelman TG, Fuchs BM. 2019. On-site analysis of bacterial communities of the Ultraoligotrophic South Pacific Gyre. *Appl Environ Microbiol* 85:e00184-19. <https://doi.org/10.1128/AEM.00184-19>
30. Osterholz H, Kilgour DPA, Storey DS, Lavik G, Ferdelman TG, Niggemann J, Dittmar T. 2021. Accumulation of DOC in the South Pacific subtropical gyre from a molecular perspective. *Marine Chem* 231:103955. <https://doi.org/10.1016/j.marchem.2021.103955>
31. Reintjes G, Fuchs BM, Amann R, Arnosti C. 2020. Extensive microbial processing of polysaccharides in the South Pacific gyre via selfish uptake and extracellular hydrolysis. *Front Microbiol* 11:583158. <https://doi.org/10.3389/fmicb.2020.583158>
32. Duerschlag J, Mohr W, Ferdelman TG, LaRoche J, Desai D, Croot PL, Voß D, Zielinski O, Lavik G, Littmann S, Martínez-Pérez C, Tschitschko B, Bartlau N, Osterholz H, Dittmar T, Kuypers MMM. 2022. Niche partitioning by photosynthetic plankton as a driver of CO₂-fixation across the oligotrophic South Pacific subtropical Ocean. *ISME J* 16:465–476. <https://doi.org/10.1038/s41396-021-01072-z>
33. Schnetzer A, Moorthi SD, Countway PD, Gast RJ, Gilg IC, Caron DA. 2011. Depth matters: microbial eukaryote diversity and community structure in the Eastern North Pacific revealed through environmental gene libraries. *Deep Sea Research Part I: Ocean Res Papers* 58:16–26. <https://doi.org/10.1016/j.dsr.2010.10.003>
34. Countway PD, Gast RJ, Dennett MR, Savai P, Rose JM, Caron DA. 2007. Distinct protistan assemblages characterize the Euphotic zone and deep sea (2500 m) of the Western North Atlantic (Sargasso sea and Gulf stream). *Environ Microbiol* 9:1219–1232. <https://doi.org/10.1111/j.1462-2920.2007.01243.x>
35. Giner CR, Pernice MC, Balagué V, Duarte CM, Gasol JM, Logares R, Massana R. 2020. Marked changes in diversity and relative activity of picoeukaryotes with depth in the world ocean. *ISME J* 14:437–449. <https://doi.org/10.1038/s41396-019-0506-9>
36. Yeh Y-C, Fuhrman JA. 2022. Contrasting diversity patterns of prokaryotes and protists over time and depth at the San-Pedro ocean time series. *ISME Commun* 2:36. <https://doi.org/10.1038/s43705-022-00121-8>
37. Sunagawa S, Coelho LP, Chaffron S, Kultima JR, Labadie K, Salazar G, Djahanschiri B, Zeller G, Mende DR, Alberti A, et al. 2015. Structure and function of the global ocean microbiome. *Science* 348:1–10. <https://doi.org/10.1126/science.1261359>
38. Cohen NR, McIlvin MR, Moran DM, Held NA, Saunders JK, Hawco NJ, Brosnahan M, DiTullio GR, Lamborg C, McCrow JP, Dupont CL, Allen AE, Saito MA. 2021. Dinoflagellates alter their carbon and nutrient metabolic strategies across environmental gradients in the central Pacific ocean. *Nat Microbiol* 6:173–186. <https://doi.org/10.1038/s41564-020-00814-7>
39. Zamora-Terol S, Novotny A, Winder M. 2021. Molecular evidence of host-parasite interactions between zooplankton and Syndiniales. *Aquat Ecol* 55:125–134. <https://doi.org/10.1007/s10452-020-09816-3>
40. Clarke LJ, Bestley S, Bissett A, Deagle BE. 2019. A globally distributed Syndiniales parasite dominates the Southern ocean micro-eukaryote community near the sea-ice edge. *ISME J* 13:734–737. <https://doi.org/10.1038/s41396-018-0306-7>
41. Rizos I, Debeljak P, Finet T, Klein D, Ayata S-D, Not F, Bittner L. 2023. Beyond the limits of the unassigned protist microbiome: inferring large-scale spatio-temporal patterns of Syndiniales marine parasites. *ISME Commun* 3:16. <https://doi.org/10.1038/s43705-022-00203-7>
42. Sehein TR, Gast RJ, Pachiadaki M, Guillou L, Edgcomb VP. 2022. Parasitic infections by group II Syndiniales target selected dinoflagellate host populations within diverse protist assemblages in a model coastal pond. *Environ Microbiol* 24:1818–1834. <https://doi.org/10.1111/1462-2920.15977>
43. Yan Y, Lin T, Xie W, Zhang D, Jiang Z, Han Q, Zhu X, Zhang H. 2023. Contrasting mechanisms determine the microeukaryotic and Syndiniales community assembly in a eutrophic bay. *Microb Ecol* 86:1575–1588. <https://doi.org/10.1007/s00248-023-02175-0>
44. Guillou L, Viprey M, Chambouvet A, Welsh RM, Kirkham AR, Massana R, Scanlan DJ, Worden AZ. 2008. Widespread occurrence and genetic diversity of marine parasitoids belonging to *Syndiniales* (*Alveolata*). *Environ Microbiol* 10:3349–3365. <https://doi.org/10.1111/j.1462-2920.2008.01731.x>
45. Chambouvet A, Morin P, Marie D, Guillou L. 2008. Control of toxic marine dinoflagellate blooms by serial parasitic killers. *Science* 322:1254–1257. <https://doi.org/10.1126/science.1164387>
46. Anderson SR, Harvey EL, Campbell BJ. 2020. Temporal variability and ecological interactions of parasitic marine Syndiniales in coastal protist communities. *mSphere* 5. <https://doi.org/10.1128/mSphere.00209-20>
47. Holt CC, Boscaro V, Van Steenkiste NWL, Herranz M, Mathur V, Irwin NAT, Buckholtz G, Leander BS, Keeling PJ. 2022. Microscopic marine invertebrates are reservoirs for cryptic and diverse protists and fungi. *Microbiome* 10:161. <https://doi.org/10.1186/s40168-022-01363-3>
48. Hu SK, Connell PE, Mesrop LY, Caron DA. 2018. A hard day's night: diel shifts in microbial eukaryotic activity in the North Pacific Subtropical Gyre. *Front Mar Sci* 5:1–17. <https://doi.org/10.3389/fmars.2018.00351>
49. Hassett BT, Vonnahme TR, Peng X, Jones EBG, Heuzé C. 2020. Global diversity and geography of planktonic marine fungi. *Botanica Marina* 63:121–139. <https://doi.org/10.1515/bot-2018-0113>
50. Ettinger CL, Vann LE, Eisen JA. 2021. Global diversity and biogeography of the *Zostera marina* microbiome. *Appl Environ Microbiol* 87:e0279520. <https://doi.org/10.1128/AEM.02795-20>
51. Richards TA, Jones MDM, Leonard G, Bass D. 2012. Marine fungi: their ecology and molecular diversity. *Ann Rev Mar Sci* 4:495–522. <https://doi.org/10.1146/annurev-marine-120710-100802>
52. Bochdansky AB, Clouse MA, Herndl GJ. 2017. Eukaryotic microbes, principally fungi and labyrinthulomycetes, dominate biomass on bathypelagic marine snow. *ISME J* 11:362–373. <https://doi.org/10.1038/ismej.2016.113>
53. Orsi WD, Vuillemin A, Coskun ÖK, Rodriguez P, Oertel Y, Niggemann J, Mohrholz V, Gomez-Saez GV. 2022. Carbon assimilating fungi from surface ocean to seafloor revealed by coupled phylogenetic and stable isotope analysis. *ISME J* 16:1245–1261. <https://doi.org/10.1038/s41396-021-01169-5>
54. Buedenbender L, Kumar A, Blümel M, Kempken F, Tasdemir D. 2021. Genomics- and metabolomics-based investigation of the deep-sea sediment-derived yeast, *Rhodotorula mucilaginosa* 50-3-19/20B. *Mar Drugs* 19:14.
55. Nagahama T, Hamamoto M, Nakase T, Takami H, Horikoshi K. 2001. Distribution and identification of red yeasts in deep-sea environments around the northwest Pacific ocean. *Antonie Van Leeuwenhoek* 80:101–110. <https://doi.org/10.1023/a:1012270503751>
56. Sobol MS, Hoshino T, Delgado V, Futagami T, Kadooka C, Inagaki F, Kiel Reese B. 2023. Genome characterization of two novel deep-sea sediment fungi, *Penicillium pacificagyrus* sp. nov. and *Penicillium pacificasedimenti* sp. nov., from South Pacific gyre seafloor sediments, highlights survivability. *BMC Genomics* 24:249. <https://doi.org/10.1186/s12864-023-09320-6>
57. Ferdelman T. 2019. *Nutrient data from CTD nissen bottles from sonne expedition SO-245 "UltraPac"*. Available from: <https://doi.pangaea.de/10.1594/PANGAEA.899228>. Retrieved 26 Oct 2022.
58. Zielinski O, Henkel R, Voß D, Ferdelman TG. 2018. Physical oceanography during SONNE cruise So245 (Ultrapac). *PANGAEA*. <https://doi.org/10.1594/PANGAEA.890394>
59. Stoeck T, Bass D, Nebel M, Christen R, Jones MDM, Breiner H-W, Richards TA. 2010. Multiple marker parallel tag environmental DNA sequencing

- reveals a highly complex eukaryotic community in marine anoxic water. *Mol Ecol* 19 Suppl 1:21–31. <https://doi.org/10.1111/j.1365-294X.2009.04480.x>
60. Tedersoo L, Anslan S, Bahram M, Pöhlme S, Riit T, Liiv I, Kõljalg U, Kisand V, Nilsson H, Hildebrand F, Bork P, Abarenkov K. 2015. Shotgun metagenomes and multiple primer pair-barcode combinations of amplicons reveal biases in metabarcoding analyses of fungi. *MC* 10:1–43. <https://doi.org/10.3897/mycokeys.10.4852>
 61. Wurzbacher C, Nilsson RH, Rautio M, Peura S. 2017. Poorly known microbial taxa dominate the microbiome of permafrost thaw ponds. *ISME J* 11:1938–1941. <https://doi.org/10.1038/ismej.2017.54>
 62. Pjevac P, Hausmann B, Schwarz J, Kohl G, Herbold CW, Loy A, Berry D. 2021. An economical and flexible dual barcoding, two-step PCR approach for highly multiplexed amplicon sequencing. *Front Microbiol* 12:669776. <https://doi.org/10.3389/fmicb.2021.669776>
 63. R Core Team. 2020. R: A language and environment for statistical computing. R Foundation for Statistical Computing Vienna, Austria. Available from: <https://www.R-project.org/>
 64. Callahan BJ, Sankaran K, Fukuyama JA, McMurdie PJ, Holmes SP. 2016. Bioconductor workflow for microbiome data analysis: from raw reads to community analyses. *F1000Res* 5:1492. <https://doi.org/10.12688/f1000research.8986.2>
 65. Guillou L, Bachar D, Audic S, Bass D, Berney C, Bittner L, Boutte C, Burgaud G, de Vargas C, Decelle J, et al. 2013. The protist ribosomal reference database (PR2): a catalog of unicellular eukaryote small subunit rRNA sequences with curated taxonomy. *Nucleic Acids Res* 41:D597–604. <https://doi.org/10.1093/nar/gks1160>
 66. Nilsson RH, Larsson KH, Taylor AFS, Bengtsson-Palme J, Jeppesen TS, Schigel D, Kennedy P, Picard K, Glöckner FO, Tedersoo L, Saar I, Kõljalg U, Abarenkov K. 2019. The UNITE database for molecular identification of fungi: handling dark taxa and parallel taxonomic classifications. *Nucleic Acids Res* 47:D259–D264. <https://doi.org/10.1093/nar/gky1022>
 67. Adl SM, Bass D, Lane CE, Lukeš J, Schoch CL, Smirnov A, Agatha S, Berney C, Brown MW, Burki F, et al. 2019. Revisions to the classification, nomenclature, and diversity of eukaryotes. *J Eukaryot Microbiol* 66:4–119. <https://doi.org/10.1111/jeu.12691>
 68. Reczuga MK, Seppely CVW, Mulot M, Jassey VEJ, Buttler A, Słowińska S, Słowiński M, Lara E, Lamentowicz M, Mitchell EAD. 2020. Assessing the responses of sphagnum micro-eukaryotes to climate changes using high throughput sequencing. *PeerJ* 8:e9821. <https://doi.org/10.7717/peerj.9821>
 69. Suter EA, Pachiadaki M, Taylor GT, Edgcomb VP. 2021. Eukaryotic parasites are integral to a productive microbial food web in oxygen-depleted waters. *Front Microbiol* 12:764605. <https://doi.org/10.3389/fmicb.2021.764605>
 70. Nguyen NH, Song Z, Bates ST, Branco S, Tedersoo L, Menke J, Schilling JS, Kennedy PG. 2016. FUNGuild: an open annotation tool for parsing fungal community datasets by ecological guild. *Fungal Ecol* 20:241–248. <https://doi.org/10.1016/j.funeco.2015.06.006>
 71. McMurdie PJ, Holmes S. 2013. phyloseq: an R package for reproducible interactive analysis and graphics of microbiome census data. *PLoS One* 8:e61217. <https://doi.org/10.1371/journal.pone.0061217>
 72. Wickham H, Averick M, Bryan J, Chang W, McGowan L, François R, Grolemund G, Hayes A, Henry L, Hester J, Kuhn M, Pedersen T, Miller E, Bache S, Müller K, Ooms J, Robinson D, Seidel D, Spinu V, Takahashi K, Vaughan D, Wilke C, Woo K, Yutani H. 2019. Welcome to the tidyverse. *JOSS* 4:1686. <https://doi.org/10.21105/joss.01686>
 73. Oksanen J, Blanchet FG, Friendly M, Kindt R, Legendre P, Mcglinn D, Minchin PR, Hara RBO, Simpson GL, Solymos P, Stevens MHH, Szoecs E. 2020. Vegan: community ecology package. R package version 2.5-7. <https://CRAN.R-project.org/package=vegan>.
 74. Wickham H. 2016. Ggplot2: elegant graphics for data analysis. Springer-Verlag, New York. Available from: <http://had.co.nz/ggplot2/book>
 75. Kolde R. 2012. “Package ‘pheatmap’: pretty heatmaps”. R package version 1.0.12. <https://CRAN.R-project.org/package=pheatmap>.
 76. Gao C-H, Yu G, Cai P. 2021. ggVennDiagram: an intuitive, easy-to-use, and highly customizable R package to generate Venn Diagram. *Front Genet* 12:706907. <https://doi.org/10.3389/fgene.2021.706907>
 77. Kembel SW, Cowan PD, Helmus MR, Cornwell WK, Morlon H, Ackerly DD, Blomberg SP, Webb CO. 2010. Picante: R tools for integrating phylogenies and ecology. *Bioinformatics* 26:1463–1464. <https://doi.org/10.1093/bioinformatics/btq166>
 78. Houyun H. 2021. linkET: everything is linkable. R package version 0.0.7.1. Available from: <https://github.com/Hy4m/linkET>
 79. Smith AB. 2018. enmSdm: tools for modeling niches and distributions of species. R package version 0.9.4. Available from: <https://github.com/adamlilith/enmSdm>
 80. Hijmans RJ. 2019. geosphere: spherical trigonometry. R package version 1.5.18. Available from: <https://github.com/rspatial/geosphere>
 81. Gutiérrez-Rodríguez A, Lopes dos Santos A, Safi K, Probert I, Not F, Fernández D, Gourvil P, Bilewicz J, Hulston D, Pinkerton M, Nodder SD. 2022. Planktonic protist diversity across contrasting subtropical and subantarctic waters of the southwest Pacific. *Prog Ocean* 206:102809. <https://doi.org/10.1016/j.pocean.2022.102809>
 82. Sievers F, Wilm A, Dineen D, Gibson TJ, Karplus K, Li W, Lopez R, McWilliam H, Remmert M, Söding J, Thompson JD, Higgins DG. 2011. Fast, scalable generation of high-quality protein multiple sequence alignments using Clustal Omega. *Mol Syst Biol* 7:539. <https://doi.org/10.1038/msb.2011.75>
 83. Price MN, Dehal PS, Arkin AP. 2010. FastTree 2 - approximately maximum-likelihood trees for large alignments. *PLoS One* 5:e9490. <https://doi.org/10.1371/journal.pone.0009490>
 84. Stegen JC, Lin X, Fredrickson JK, Chen X, Kennedy DW, Murray CJ, Rockhold ML, Konopka A. 2013. Quantifying community assembly processes and identifying features that impose them. *ISME J* 7:2069–2079. <https://doi.org/10.1038/ismej.2013.93>
 85. Stegen JC, Lin X, Fredrickson JK, Konopka AE. 2015. Estimating and mapping ecological processes influencing microbial community assembly. *Front Microbiol* 6:370. <https://doi.org/10.3389/fmicb.2015.00370>